J. Appl. Math. & Informatics Vol. **28***(2010), No.5-6, pp. 1331-1345*
Website: http://www.kcam.biz

A MIXED FINITE ELEMENT METHOD FOR NAVIER-STOKES EQUATIONS

ABDESLAM ELAKKAD*, AHMED ELKHALFI AND NAJIB GUESSOUS

Abstract. This paper describes a numerical solution of Navier-Stokes equations. It includes algorithms for discretization by finite element methods and a posteriori error estimation of the computed solutions. In order to evaluate the performance of the method, the numerical results are compared with some previously published works or with others coming from commercial code like ADINA system.

AMS Mathematics Subject Classification : 65F10, 65F05.
Key words and phrases : Incompressible Navier-Stokes Equations, Mixed Finite Element Method, A posteriori error estimates, Iterative solvers, Adina system.

1. Introduction

A posteriori error analysis in problems related to fluid dynamics is a subject that has received a lot of attention during the last decades. In the conforming case there are several ways to define error estimators by using the residual equation. In particular, for the Stokes problem, M. Ainsworth, J. Oden [1], R.E. Bank, B.D. Welfert [3], C. Carstensen, S.A. Funken [6], and R. Verfurth [16] introduced several error estimators and provided that they are equivalent to the energy norm of the errors. Other works for the stationary Navier-Stokes problem have been introduced in [12, 14, 17, 18].
This paper describes a numerical solutions of partial differential equations (PDEs) that are used to model steady incompressible fluid flow. It is structured as a stand-alone package for studying discretization algorithms for PDEs and for exploring and developing algorithms in numerical linear and nonlinear algebra for solving the associated discrete systems. It can also be used as a pedagogical tool for studying these issues, or more elementary ones such as the properties of Krylov subspace iterative methods. The latter two PDEs constitute the basis

Received March 5, 2010. Revised March 16, 2010. Accepted May 27, 2010. *Corresponding author.

for computational modeling of the flow of an incompressible Newtonian fluid.
For the equations , we offer a choice of two-dimensional domains on which the problem can be posed, along with boundary conditions and other aspects of the problem, and a choice of finite element discretizations on a quadrilateral element mesh. whereas the discrete Navier-Stokes equations require a method such as the generalized minimum residual method (GMRES) , which is designed for non symmetric systems [7]. The key for fast solution lies in the choice of effective preconditioning strategies. The package offers a range of options, including algebraic methods such as incomplete LU factorizations, as well as more sophisticated and state-of-the-art multigrid methods designed to take advantage of the structure of the discrete linearized Navier-Stokes equations. In addition, there is a choice of iterative strategies, Picard iteration or Newton's method, for solving the nonlinear algebraic systems arising from the latter problem.
Section 2 presents the model problem used in this paper. The discretization by mixed finite elements described is in section 3. Section 4 shows the methods of a posteriori error bounds of the computed solution. Numerical experiments carried out within the framework of this publication and their comparisons with other results are shown in section 5.

2. INCOMPRESSIBLE NAVIER-STOKES EQUATIONS

We consider the steady-state Navier-Stokes equations for the flow of a Newtonian incompressible viscous fluid with constant viscosity:

$$\begin{cases} -\nu\nabla^2\overrightarrow{u} + \overrightarrow{u}.\nabla\overrightarrow{u} + \nabla p = \overrightarrow{f}, \\ \nabla.\overrightarrow{u} = 0, \end{cases} \tag{1}$$

where $\nu > 0$ is a given constant called the kinematic viscosity.
$\overrightarrow{u}$ is the fluid velocity, p is the pressure field, and ∇ is the gradient and $\nabla.$ is the divergence operator.
The boundary value problem that is considered is the system (1) posed on two or three-dimensional domain Ω, together with boundary conditions on $\partial\Omega = \partial\Omega_D \bigcup \partial\Omega_N$ given by

$$\overrightarrow{u} = \overrightarrow{W} \text{ on } \partial\Omega_D, \quad \nu\frac{\partial\overrightarrow{u}}{\partial n} - \overrightarrow{n}p = \overrightarrow{0} \text{ on } \partial\Omega_N, \tag{2}$$

where $\overrightarrow{n}$ denote the outward pointing normal to the boundary.
This system is the basis for computational modeling of the flow of an incompressible Newtonian fluid such as air or water. The presence of the nonlinear convection term $\overrightarrow{u}.\nabla\overrightarrow{u}$ means that boundary value problems associated with the Navier-Stokes equations can have more than one solution.
Mixed finite element discretization of the weak formulation of the Navier- Stokes equations gives rise to a nonlinear system of algebraic equations. Two classical iterative procedures for solving this system are Newton iteration and Picard iteration.

We define the spaces

$$\hbar^1(\Omega) = \{u : \Omega \to IR/u, \tfrac{\partial u}{\partial x}, \tfrac{\partial u}{\partial y} \in L_2(\Omega)\} \tag{3}$$

$$H_E^1 = \{\overrightarrow{u} \in \hbar^1(\Omega)^d / \overrightarrow{u} = \overrightarrow{W} \text{ on } \partial\Omega_D\} \tag{4}$$

$$H_{E_0}^1 = \{\overrightarrow{v} \in \hbar^1(\Omega)^d / \overrightarrow{v} = \overrightarrow{0} \text{ on } \partial\Omega_D\}. \tag{5}$$

Then the standard weak formulation of the Navier-Stokes flow problem (1) and (2) is the following:
Find $\overrightarrow{u} \in H_E^1$ and $p \in L_2(\Omega)$ such that

$$\nu \int_\Omega \nabla\overrightarrow{u}.\nabla\overrightarrow{v} + \int_\Omega (\overrightarrow{u}.\nabla\overrightarrow{u}).\overrightarrow{v} - \int_\Omega p(\nabla.\overrightarrow{v}) = \int_\Omega f.\overrightarrow{v}, \text{ for all } \overrightarrow{v} \in H_{E_0}^1 \tag{6}$$

$$\int_\Omega q(\nabla.\overrightarrow{u}) = 0 \text{ for all } q \in L_2(\Omega). \tag{7}$$

Let the trilinear form
$c : H_{E_0}^1 \times H_{E_0}^1 \times H_{E_0}^1 \longrightarrow \mathbb{R}$ defined as follows:

$$c(\overrightarrow{z}; \overrightarrow{u}, \overrightarrow{v}) = \int_\Omega (\overrightarrow{z}.\nabla\overrightarrow{u}).\overrightarrow{v}. \tag{8}$$

The convection term is skew-symmetric: $c(\overrightarrow{z}; \overrightarrow{u}, \overrightarrow{v}) = -c(\overrightarrow{z}; \overrightarrow{v}, \overrightarrow{u})$.
Establishing continuity, that is,

$$c(\overrightarrow{z}; \overrightarrow{u}, \overrightarrow{v}) \leq \Gamma \| \bigtriangledown \overrightarrow{z} \| \, \| \bigtriangledown \overrightarrow{u} \| \, \| \bigtriangledown \overrightarrow{v} \|, \tag{9}$$

see Girault δ Raviart [10, p. 284].
We define

$$V_{E_0} = \{\overrightarrow{z} \in H_{E_0}^1; \nabla.\overrightarrow{z} = 0 \text{ in } \Omega\}, \tag{10}$$

$$\| \overrightarrow{f} \|_* = \sup_{\overrightarrow{v} \in V_{E_0}} \frac{(\overrightarrow{f}, \overrightarrow{v})}{\|\nabla\overrightarrow{v}\|}.$$

Then a well-known (sufficient) condition for uniqueness (see [10, Theorem 2.2]) is that forcing function is small in the sense that

$$\| \overrightarrow{f} \|_* \leq \frac{\nu^2}{\Gamma_*}, \tag{11}$$

where Γ_* is the best possible constant such that (9) holds.

3. Mixed finite element approximation

A discrete weak formulation is defined using finite dimensional spaces $X_0^h \subset H_{E_0}^1$ and $M^h \subset L_2(\Omega)$. Specifically, given a velocity solution spaces X_E^h, the discrete version of (6)-(7) is:
find $\overrightarrow{u}_h \in X_E^h$ and $p_h \in M^h$ such that

$$\nu \int_\Omega \nabla\overrightarrow{u}_h.\nabla\overrightarrow{v}_h + \int_\Omega (\overrightarrow{u}_h.\nabla\overrightarrow{u}_h).\overrightarrow{v}_h - \int_\Omega p_h(\nabla.\overrightarrow{v}_h) = \int_\Omega \overrightarrow{f}.\overrightarrow{v}_h, \tag{12}$$

$$\int_\Omega q_h(\nabla.\overrightarrow{u}_h) = 0, \tag{13}$$

for all $\overrightarrow{v}_h \in X_0^h$ and $q_h \in M^h$.
We define the appropriate bases for the finite element spaces, leading to a non linear system of algebraic equations. Linearization of this system using Newton iteration gives the finite dimensional system: find $\delta\overrightarrow{u}_h \in X_0^h$ and $\delta p_h \in M^h$ such that

$$c(\delta\overrightarrow{u}_h;\overrightarrow{u}_h,\overrightarrow{v}_h) + c(\overrightarrow{u}_h;\delta\overrightarrow{u}_h,\overrightarrow{v}_h) + \nu\int_\Omega \nabla\delta\overrightarrow{u}_h.\nabla\overrightarrow{v}_h - \int_\Omega \delta p_h(\nabla.\overrightarrow{v}_h) = R_k(\overrightarrow{v}_h),$$

$$\int_\Omega q_h(\nabla.\delta\overrightarrow{u}_h) = r_k(q_h), \tag{14}$$

for all $\overrightarrow{v}_h \in X_0^h$ and $q_h \in M^h$. Here, $R_k(\overrightarrow{v}_h)$ and $r_k(q_h)$ are the non linear residuals associated with the discrete formulations (12) and(13).
We use a set of vector-valued basis functions $\{\overrightarrow{\varphi}_j\}$, so that

$$\overrightarrow{u}_h = \sum_1^{n_u} u_j\overrightarrow{\varphi}_j + \sum_{n_u+1}^{n_u+n_\partial} u_j\overrightarrow{\varphi}_j,\ \delta\overrightarrow{u}_h = \sum_{j=1}^{n_u}\Delta u_j\overrightarrow{\varphi}_j, \tag{15}$$

and we fix the coefficients $u_j : j = n_u + 1, \ldots, n_u + n_\partial$, so that the second term interpolates the boundary data on $\partial\Omega_D$.
We introduce a set of pressure basis functions $\{\Psi_k\}$ and set

$$p_h = \sum_{k=1}^{n_p} p_k\Psi_k,\ \delta p_h = \sum_{k=1}^{n_p}\Delta p_k\Psi_k, \tag{16}$$

where n_u and n_p are the numbers of velocity and pressure basis functions, respectively.
We obtain a system of linear equations

$$\begin{pmatrix} \nu A + N + W & {}^tB \\ B & 0 \end{pmatrix}\begin{pmatrix} \Delta U \\ \Delta P \end{pmatrix} = \begin{pmatrix} f \\ g \end{pmatrix}. \tag{17}$$

This system is referred to as the discrete Newton problem.
The matrix A is the vector Laplacian matrix and B is the divergence matrix

$$A = [a_{ij}],\ a_{ij} = \int_\Omega \nabla\overrightarrow{\varphi}_i.\nabla\overrightarrow{\varphi}_j, \tag{18}$$

$$B = [b_{kj}],\ b_{kj} = -\int_\Omega \Psi_k\nabla.\overrightarrow{\varphi}_j, \tag{19}$$

for i and j=1, . . . , n_u and k=1, . . . , n_p.
The vector-convection matrix N and the Newton derivative matrix W are given by

$$N = [n_{ij}],\ n_{ij} = \int_\Omega (\overrightarrow{u}_h.\nabla\overrightarrow{\varphi}_j).\overrightarrow{\varphi}_i, \tag{20}$$

$$W = [W_{ij}],\ W_{ij} = \int_\Omega (\overrightarrow{\varphi}_j.\nabla\overrightarrow{u}_h).\overrightarrow{\varphi}_i, \tag{21}$$

for i and j=1, . . . , n_u. The Newton derivative matrix is symmetric.
The right-hand side vectors in (17) are the non linear residuals associated with the current discrete solution $\overrightarrow{u}_h$ and p_h.

$$f = [f_i],\ f_i = \int_\Omega f.\overrightarrow{\varphi}_i - \int_\Omega (\overrightarrow{u}_h.\nabla\overrightarrow{u}_h).\overrightarrow{\varphi_i} - \nu\int_\Omega \nabla\overrightarrow{u}_h.\nabla\overrightarrow{\varphi}_i + \int_\Omega p_h(\nabla.\overrightarrow{\varphi}_i) \tag{22}$$

$$g = [g_k],\ g_k = -\int_\Omega (\Psi_k.\nabla.\overrightarrow{u}_h). \tag{23}$$

For Picard iteration we give the discrete problem

$$\begin{pmatrix} \nu A + N & {}^tB \\ B & 0 \end{pmatrix}\begin{pmatrix} \Delta U \\ \Delta P \end{pmatrix} = \begin{pmatrix} f \\ g \end{pmatrix}. \tag{24}$$

The lowest order mixed approximations like $Q_1 - P_0$ and $Q_1 - Q_1$ are unstable. The discrete approximation is stabilised by replacing the zero block in the Newton system (17) and the system (24) with stabilisation matrix.
The stabilized analogue of the system (24) is given by

$$\begin{pmatrix} \nu A + N & {}^tB \\ B & -\frac{1}{\nu}C \end{pmatrix}\begin{pmatrix} U \\ P \end{pmatrix} = \begin{pmatrix} f \\ g \end{pmatrix}, \tag{25}$$

where C is the Stokes stabilization matrix in the case of $Q_1 - P_0$ or $Q_1 - Q_1$ mixed approximation, and is the zero matrix otherwise.
For the stokes problem the stabilization matrix is $C = \frac{1}{4}diag[C^*, \ldots, C^*]$ with C^* is given by

$$C^* = h_x h_y \begin{pmatrix} 2 & -1 & 0 & -1 \\ -1 & 2 & -1 & 0 \\ 0 & -1 & 2 & -1 \\ -1 & 0 & -1 & 2 \end{pmatrix}. \tag{26}$$

We use a stabilized element pair $Q_1 - P_0$, This is the most famous example of an unstable element pair, using bilinear approximation for velocity and a constant approximation for the pressure.
We use two iterative methods for solving the nonsymmetric systems: The generalized minimum residual method (GMRES) and BiConjugate Gradients Stabilized Method (BICGSTAB).
Preconditioning is a technique used to enhance the convergence of an iterative method to solve a large linear systems iteratively. Instead of solving a system $\Lambda x = b$, one solves a system $P^{-1}\Lambda x = P^{-1}b$, where P is the preconditioner. A good preconditioner should lead to fast convergence of the Krylov method. Furthermore, systems of the form Pz = r should be easy to solve.
For the Navier-Stokes equations, the objective is to design a preconditioner, that increases the convergence of an iterative method independent of the Reynolds number and number of gridpoints. We use a least-squares commutator preconditioning [15].

4. A posteriori error bounds

We restrict of enclosed flow with $\partial\Omega = \partial\Omega_D$ and $\overrightarrow{W} = \overrightarrow{0}$.

A clever choice (due to R. E. Bank, A. Weiser [2]) is the correction space

$$\Theta_T = Q_T \oplus B_T$$

consisting of edge and interior bubble functions, respectively;

$$Q_T = span\{\psi_E : E \in \varepsilon(T) \cap (\varepsilon_{h,\Omega} \cup \varepsilon_{h,N})\},$$

where $\psi_E : T \to \mathbb{R}$ is the quadratic (or biquadratic) edge-bubble that is zero on the other two (or three) edges of T (see ([17, pages 9-10]). B_T is the space spanned by interior cubic (or biquadratic) bubbles ϕ_T such that $0 \leq \phi_T \leq 1$, $\phi_T = 0$ on ∂T and $\phi_T = 1$ only at the centroid.
Let the continuous bilinear forms $a : H^1 \times H^1 \longrightarrow \mathbb{R}$ and $b : H^1 \times L_2(\Omega) \longrightarrow \mathbb{R}$
$a(\overrightarrow{u}, \overrightarrow{v}) = \nu \int_\Omega \nabla\overrightarrow{u}.\nabla\overrightarrow{v}$, $b(\overrightarrow{v}, q) = -\int_\Omega q(\nabla.\overrightarrow{v})$.
Given the continuous functional $l : H^1 \longrightarrow \mathbb{R}$
$l(\overrightarrow{v}) = \int_\Omega \overrightarrow{f}.\overrightarrow{v}$;
the underlying weak formulation (6)-(7) may be restated as
Find $\overrightarrow{u} \in H^1_{E_0}$ and $p \in L_2(\Omega)$ such that

$$\begin{cases} a(\overrightarrow{u}, \overrightarrow{v}) + c(\overrightarrow{u}; \overrightarrow{u}, \overrightarrow{v}) + b(\overrightarrow{v}, p) = l(\overrightarrow{v}), \text{ for all } \overrightarrow{v} \in H^1_{E_0} \\ b(\overrightarrow{u}, q) = 0, \text{ for all } q \in L_2(\Omega). \end{cases} \tag{27}$$

With a conforming mixed approximation, the corresponding discrete problem (13)-(14) is given by Find $\overrightarrow{u}_h \in X^h_0$ and $p_h \in M^h$ such that:

$$\begin{cases} a(\overrightarrow{u}_h, \overrightarrow{v}_h) + c(\overrightarrow{u}_h; \overrightarrow{u}_h, \overrightarrow{v}_h) + b(\overrightarrow{v}_h, p_h) = l(\overrightarrow{v}_h), \text{ for all } \overrightarrow{v}_h \in X^h_0, \\ b(\overrightarrow{u}_h, q_h) = 0, \text{ for all } q_h \in M^h. \end{cases} \tag{28}$$

Our aim is to bound $\|\overrightarrow{u} - \overrightarrow{u}_h\|_X$ and $\|p - p_h\|_M$ with respect to the energy norm for the velocity $\|\overrightarrow{v}\|_X = \|\nabla\overrightarrow{v}\|$ and the quotient norm for the pressure $\|p\|_M = \|p\|_{0,\Omega}$.
Let the symmetric bilinear form

$$B((\overrightarrow{u}, p); (\overrightarrow{v}, q)) = a(\overrightarrow{u}, \overrightarrow{v}) + b(\overrightarrow{u}, q) + b(\overrightarrow{v}, p),$$

the continuous B-stability constant

$$\sup_{(\overrightarrow{v},q)\in H^1_{E_0}\times L_2(\Omega)} \frac{B((\overrightarrow{w}, s); (\overrightarrow{v}, q))}{(\|\nabla\overrightarrow{v}\|^2 + \|q\|^2_{0,\Omega})^{\frac{1}{2}}} \geq \gamma(\|\nabla\overrightarrow{w}\|^2) + \|s\|^2_{0,\Omega})^{\frac{1}{2}}. \tag{29}$$

Given such a macroelement partitioning, say T_M, the discrete incompressibility constraint in (28) is

$$b(\overrightarrow{u}_h, q_h) - \frac{1}{4} \sum_{T\in T_M} |M| \sum_{e\in\Gamma_M} \langle [[p_h]]_e, [[q_h]]_e \rangle_{\overline{E}} = 0, \tag{30}$$

for all $q_h \in M^h$(*see*[13]), here, $|M|$ is the mean element area within the macroelement M, the set Γ_M consists of interior element edges in M, $[[p_h]]_e$ is the jump across edge e, and $\langle p, q\rangle_{\overline{E}} = \int_E pq$,

and introducing the functional $F((\overrightarrow{v},q)) = l(\overrightarrow{v})$ associated with the forcing term, we have that the errors $\overrightarrow{e} = \overrightarrow{u} - \overrightarrow{u_h} \in H^1_{E_0}$ and $\varepsilon = p - p_h \in L_2(\Omega)$ associated with (27) and (28) satisfy

$$\begin{aligned} B((\overrightarrow{e},\varepsilon);(\overrightarrow{v},q)) &= B((\overrightarrow{u}-\overrightarrow{u}_h, p-p_h);(\overrightarrow{v},q)) \\ &= B((\overrightarrow{u},p);(\overrightarrow{v},q)) - B((\overrightarrow{u}_h,p_h);(\overrightarrow{v},q)) \\ &= F((\overrightarrow{v},q)) - c(\overrightarrow{u};\overrightarrow{u},\overrightarrow{v}) - B((\overrightarrow{u}_h,p_h);(\overrightarrow{v},q)) \\ &= -c(\overrightarrow{u};\overrightarrow{u},\overrightarrow{v}) + l(\overrightarrow{v}) - a(\overrightarrow{u}_h,\overrightarrow{v}) - b(\overrightarrow{v},p_h) - b(\overrightarrow{u}_h,q), \end{aligned}$$

for all $(\overrightarrow{v},q) \in H^1_{E_0} \times L_2(\Omega)$.
We note that

$$\begin{aligned} D(\overrightarrow{u}_h,\overrightarrow{e},\overrightarrow{v}) &= c(\overrightarrow{e}+\overrightarrow{u}_h;\overrightarrow{e}+\overrightarrow{u}_h,\overrightarrow{v}) - c(\overrightarrow{u}_h;\overrightarrow{u}_h,\overrightarrow{v}) \\ &= c(\overrightarrow{u};\overrightarrow{u},\overrightarrow{v}) - c(\overrightarrow{u}_h;\overrightarrow{u}_h,\overrightarrow{v}). \end{aligned} \tag{31}$$

We get

$$\begin{aligned} &B((\overrightarrow{e},\varepsilon);(\overrightarrow{v},q)) + D(\overrightarrow{u}_h,\overrightarrow{e},\overrightarrow{v}) \\ &= -c(\overrightarrow{u}_h;\overrightarrow{u}_h,\overrightarrow{v}) + l(\overrightarrow{v}) - a(\overrightarrow{u}_h,\overrightarrow{v}) - b(\overrightarrow{v},p_h) - b(\overrightarrow{u}_h,q). \end{aligned}$$

We define the equidistributed stress jump operator

$$\overrightarrow{R}^*_E = \frac{1}{2}[[\nu\nabla\overrightarrow{u}_h - p_h\overrightarrow{I}]], \tag{32}$$

and the interior residuals $\overrightarrow{R}_T = \{\overrightarrow{f} + \nu\nabla^2\overrightarrow{u}_h - \overrightarrow{u}_h.\nabla\overrightarrow{u}_h - \nabla p_h\}/T$, and $R_T = \{\nabla.\overrightarrow{u}_h\}/T$, we find that the errors $\overrightarrow{e} \in H^1_{E_0}$ and $\varepsilon \in L_2(\Omega)$ satisfy the non linear equation

$$\begin{aligned} B((\overrightarrow{e},\varepsilon);(\overrightarrow{v},q)) + D(\overrightarrow{u}_h,\overrightarrow{e},\overrightarrow{v}) = \sum_{T\in\tau_h}\Big[(\overrightarrow{R}_T,\overrightarrow{v})_T - \sum_{E\in\varepsilon(T)} <\overrightarrow{R}^*_E,\overrightarrow{v}>_E \\ + (R_T,q)_T\Big], \end{aligned} \tag{33}$$

for all $(\overrightarrow{v},q) \in H^1_{E_0} \times L_2(\Omega)$.
The error characterization (33) is the starting point for a posteriori error analysis. The crucial question here is to determine the best way of handling the non linear term on the left-hand side of (33).
We note that
$D(\overrightarrow{u}_h,\overrightarrow{e},\overrightarrow{v}) = c(\overrightarrow{e};\overrightarrow{e},\overrightarrow{v}) + c(\overrightarrow{e};\overrightarrow{u}_h,\overrightarrow{v}) + c(\overrightarrow{u}_h;\overrightarrow{e},\overrightarrow{v})$.
The problem (33) can be approximated by the linear problem: find $\overrightarrow{e} \in H^1_{E_0}$ and $\varepsilon \in L_2(\Omega)$ such that

$$\begin{aligned} &c(\overrightarrow{e};\overrightarrow{u}_h,\overrightarrow{v}) + c(\overrightarrow{u}_h;\overrightarrow{e},\overrightarrow{v}) + \nu\int_\Omega \nabla\overrightarrow{e}.\nabla\overrightarrow{v} - \int_\Omega \varepsilon(\nabla.\overrightarrow{v}) \\ &= \sum_{T\in\tau_h}[(\overrightarrow{R}_T,\overrightarrow{v})_T - \sum_{E\in\varepsilon(T)} <\overrightarrow{R}^*_E,\overrightarrow{v}>_E] - \int_\Omega q(\nabla.\overrightarrow{e}) = \sum_{T\in\tau_h}(R_T,q)_T. \end{aligned} \tag{34}$$

This system corresponds to a Newton linearization about the discrete velocity solution $\overrightarrow{u}_h$.

We shall concentrate on the stabilized $Q_1 - P_0$ or $P_1 - P_0$ approximation methods in two dimensions. Notice that for either of these low order approximations, the divergence residual R_T is piecewise constant and the stress jump term $\overrightarrow{R}_E^*$ is piecewise linear. The other element residual is given by $\overrightarrow{R}_T = \{\overrightarrow{f} - \overrightarrow{u}_h.\nabla\overrightarrow{u}_h\}/T$.
We introduce the higher order approximation space $\Theta_T = (Q_T)^2$ for the two velocity components and compute the element function $\overrightarrow{e}_T \in \Theta_T$ satisfying the uncoupled poisson problems

$$\nu(\nabla\overrightarrow{e}_T, \nabla\overrightarrow{v})_T = (\overrightarrow{R}_T, \overrightarrow{v})_T - \sum_{E\in\varepsilon(T)} < \overrightarrow{R}_E^*, \overrightarrow{v} >_E, \text{ for all } \overrightarrow{v} \in \Theta_T. \quad (35)$$

With $\varepsilon_T = \nabla.\overrightarrow{u}_h$, the local error estimator is given by the combination of the 'energy norm' of the velocity error and the L_2 norm of the element divergence error, that is

$$\eta_T^2 = \|\nabla\overrightarrow{e}_T\|_T^2 + \|\varepsilon_T\|_T^2 = \|\nabla\overrightarrow{e}_T\|_T^2 + \|\nabla.\overrightarrow{u}_h\|_T^2, \quad (36)$$

and the global error estimator is : $\eta = (\sum_{T\in\tau_h}\eta_T^2)^{\frac{1}{2}}$
Given a rectangular element, with horizontal and vertical edges of lengths h_x, and h_y respectively.
The rectangle aspect ratio $\beta_T = \max\{h_x/h_y, h_y/h_x\}$.

Definition 1. (Aspect ratio condition).
A sequence of rectangular grids $\{\tau_h\}$ is said to be shape regular if there exists a maximum rectangle edge ratio β_* such that every element in τ_h satisfies
$1 \leq \beta_T \leq \beta_*$.

Proposition. Let condition (11) be satisfied so that there exists a unique solution $(\overrightarrow{u}, p)$ to the variational problem (27) in the enclosed flow case $\overrightarrow{u} = \overrightarrow{0}$ on $\partial\Omega$. If the discrete problem (28) is solved using a grid of $Q_1 - P_0$ rectangular elements with a pressure jump stabilization in (30), then the estimator η_T in (35) satisfies the upper bound

$$\|\nabla(\overrightarrow{u} - \overrightarrow{u}_h)\| + \|p - p_h)\|_{0,\Omega} \leq C(\sum_{T\in\tau_h}\eta_T^2)^{\frac{1}{2}}, \quad (37)$$

where C depends only on the aspect ratio constant given in definition 1 and the continuous B-stability constant in (29).

5. Numerical simulation

In this section some numerical results of calculations with Mixed finite element Method and ADINA system will be presented. Using our solver, We run two traditional test problems (driven cavity flow [4, 7, 8, 9, 19] and L-shaped domain [11, 15]) with a number of different model parameters. We can introduce by increasing Reynold's number, and we discuss the performance of our code.

Example 1. Square domain, regularized cavity boundary condition.
This is a classic test problem used in fluid dynamics, known as driven-cavity flow. It is a model of the flow in a square cavity with the lid moving from left to right. Let the computational model:
$\{y = 1; -1 \leq x \leq 1/u_x = 1 - x^4\}$, a regularized cavity.
The streamlines are computed from the velocity solution by solving the poisson equation numerically subject to a zero Dirichlet boundary condition.
We have solved the problem for three different Reynold's numbers: 100, 600, and 2000.

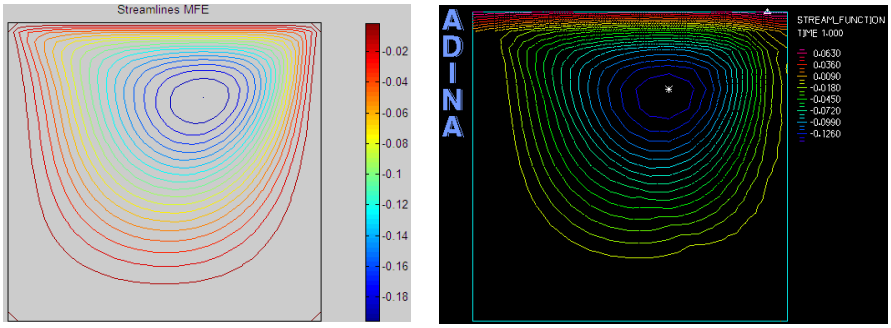

Fig.1. Uniform streamline plot (left) associated with a 64×64 square grid of a $Q_1 - Q_0$ approximation, and uniform streamline plot(right) computed with ADINA system, with Reynold number $Re = 100$.

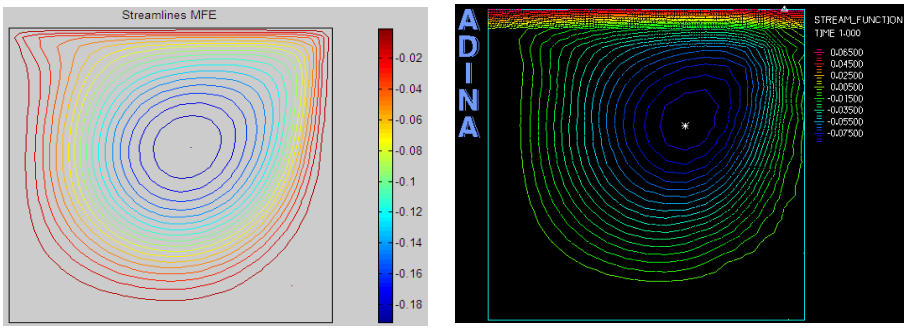

Fig.2. Uniform streamline plot (left) associated with a 64×64 square grid of a $Q_1 - Q_0$ approximation, and uniform streamline plot(right) computed with ADINA system, with Reynold number $Re = 600$.

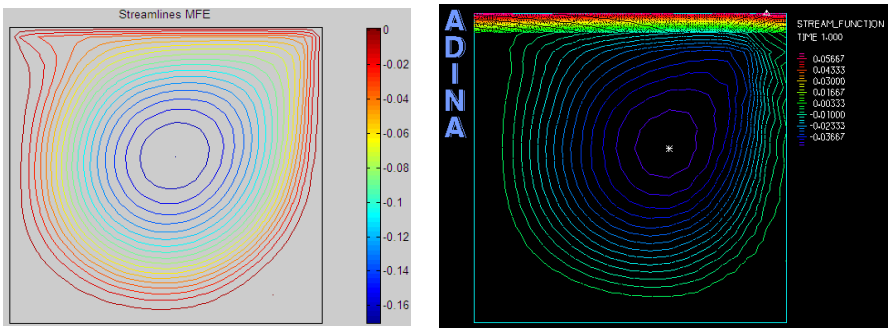

Fig.3. Uniform streamline plot (left) associated with a 64×64 square grid of a $Q_1 - Q_0$ approximation, and uniform streamline plot(right) computed with ADINA System, with Reynold number $Re = 2000$.

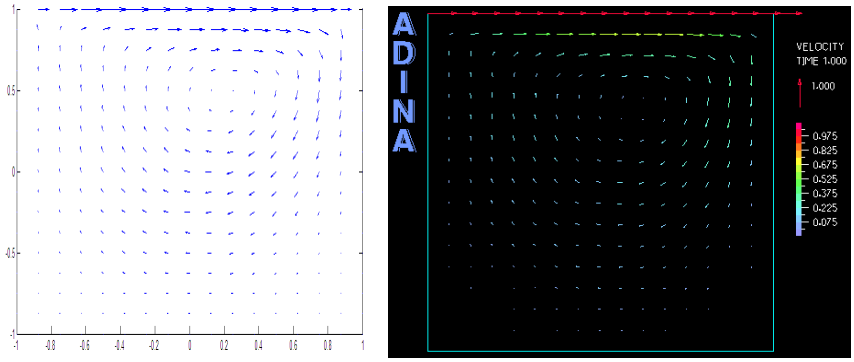

Fig.4. Velocity vectors solution by MFE (left) and velocity vectors solution (right) computed with ADINA system with a 64×64 square grid and $Re = 100$.

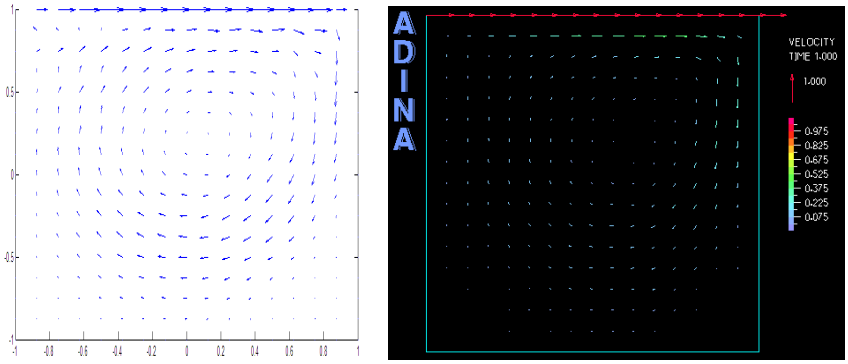

Fig.5. Velocity vectors solution by MFE (left) and velocity vectors solution (right) computed with ADINA system with a 64×64 square grid and $Re = 600$.

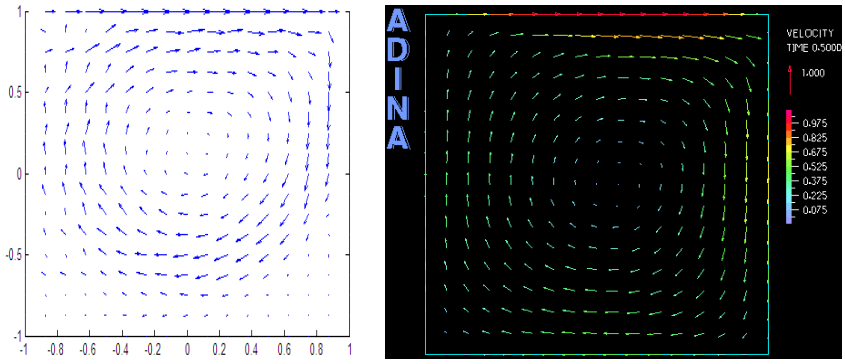

Fig.6. Velocity vectors solution by MFE (left) and velocity vectors solution (right) by ADINA system with a 64×64 square grid and $Re = 2000$.

The solution shown in figure 3 corresponds to a Reynolds number of 2000. The particles in the body of the fluid move in a circular trajectory. Steady flow in a two dimensional cavity is not stable for Reynolds number much greater than 10^4. Indeed, we have made calculations for Reynolds number 10^4, in addition, our code does not converge because the turbulence phenomena is not taken into account in our model.

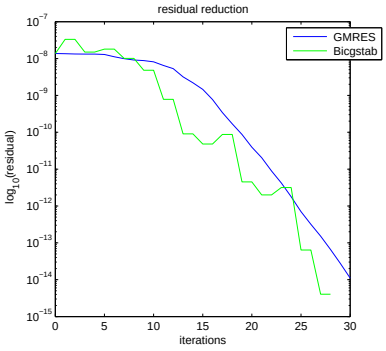

Fig.7. Iteration counts for GMRES and Bicgstab with least-squares commutator preconditioning.

Table 1. Estimated errors for regularized driven cavity flow using $Q_1 - P_0$ approximation for the flow with Reynolds number $Re = 100$.$\|\nabla . \overrightarrow{u}_h\|_\Omega$ estimated velocity divergence error. η the global error estimator.

	$\|\nabla . \overrightarrow{u}_h\|_\Omega$	η
8×8	8.704739e-002	1.720480e+000
16×16	3.115002e-002	1.084737e+000
32×32	9.545524e-003	5.919904e-001
64×64	2.676623e-003	3.160964e-001

Table 2. CPU time in seconds for the different approximations with various coarse meshes.

	$Q_1 - P_0$	$Q_1 - Q_1$	$Q_2 - Q_1$	$Q_2 - P_1$
8×8	1.2344	0.9375	1.1406	1.2188
16×16	1.8281	1.2813	1.7031	1.7188
32×32	4.3281	3.1250	3.5938	4.1094
64×64	18.7656	15.4688	23.2969	26.1250

Example 2. L-shaped domain Ω, parabolic inflow boundary condition, natural outflow boundary condition.
This example represents flow in a rectangular duct with a sudden expansion; a Poiseuille flow profile is imposed on the inflow boundary (x=-1; $0 \leq y \leq 1$), and a no-flow (zero velocity) condition is imposed on the walls. The Neumann condition (37) is applied at the outflow boundary (x=5; $-1 < y < 1$) and automatically sets the mean outflow pressure to zero.

$$\begin{cases} \nu \frac{\partial u_x}{\partial x} - p = 0 \\ \frac{\partial u_y}{\partial x} = 0 \end{cases} \tag{38}$$

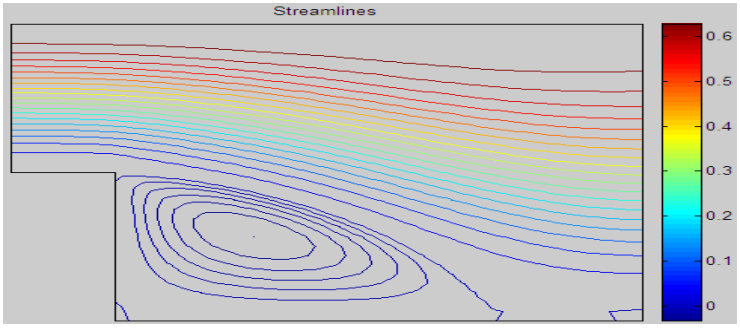

Fig.8. Equally spaced streamline plot associated with a 32×96 square grid $Q_1 - P_0$ approximation and $\nu = 1/100$.

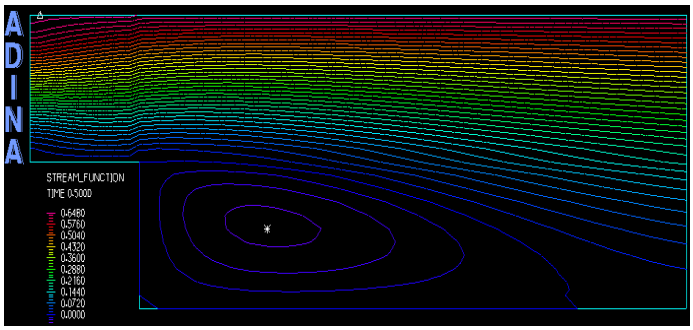

Fig.9. The solution computed with ADINA system. The plots show the streamlines associated with a 32×96 square grid and $\nu = 1/100$.

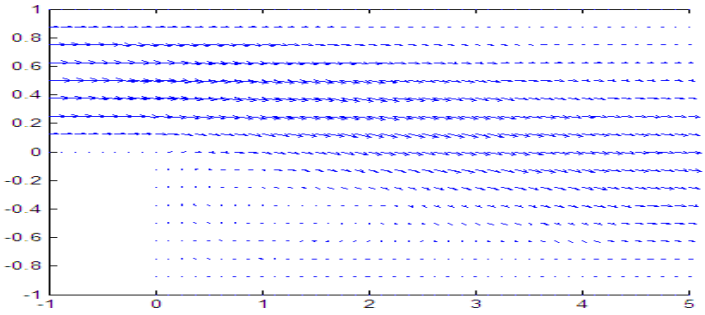

Fig.10. Velocity vectors solution by MFE, with a 32×96 square grid and $\nu = 1/100$.

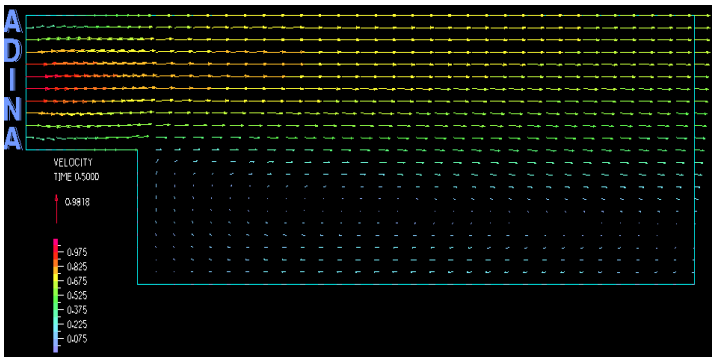

Fig.11. The solution computed with ADINA system. The plots show the velocity vectors solution with a 32×96 square grid and $\nu = 1/100$.
The two solutions are therefore essentially identical. This is very good indication that my solver is implemented correctly.

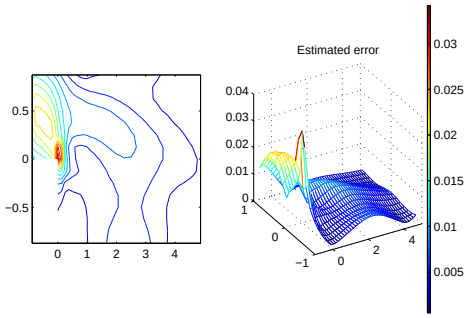

Fig.12. Estimated error η_T associated with 32×96, square grid of a $Q_1 - Q_0$ solution for the flow with $\nu = 1/100$.

The increased velocity caused by convection makes it harder for the fluid to flow around the corner, and a slow-moving component of the fluid becomes entrained behind the step.There are two sets of streamlines at equally spaced levels plotted in figure 8; one set is associated with positive treamfunction values and shows the path of particles introduced at the inflow. these pass over the step and exit at the outflow. The second set of streamlines is associated with negative values of the streamfunction. These streamlines show the path of particles in the recirculation region near the step; they are much closer in value, reflecting the fact that recirculating flow is relatively slow-moving.
If L is taken to be the height of the outflow region,then the flow pattern shown in figure 8 corresponds to a Reynolds number of 100. If the viscosity parameter were an order of magnitude smaller, then the steady flow would be unstable. The singularity at the origin is an important feature of the flow even in the convection-dominated case.

6. Conclusion

We were interested in this work in the numeric solution for two dimensional partial differential equations modeling (or arising from) model steady incompressible fluid flow. It includes algorithms for discretization by mixed finite element methods and a posteriori error estimation of the computed solutions. For the test of driven-cavity flow, the particles in the body of the fluid move in a circular trajectory. Steady flow in a two dimensional cavity is not stable for Reynolds number much greater than 10^4.
Our results agree with Adina system.
Numerical results are presented to see the performance of the method, and seems to be interesting by comparing them with other recent results.

ACKNOWLEDGMENT

The authors would like to express their sincere thanks for the referee for his/her helpful suggestions.

References

1. M. Ainsworth, J. Oden, *A posteriori error estimates for Stokes and Oseen equations*, SIAM J. Numer. Anal **34** (1997), 228-245.
2. Bank, A. Weiser, *Some a posteriori error estimators for elliptic partial differential equations*, Math. Comp **44**(1985), 283-301.
3. E. Bank, B. D. Welfert, *A posteriori error estimates for the Stokes problem*, SIAM J. Numer. Anal **28** (1991), 309-325.
4. E. Barragy, G. F. Carey, *Stream function-vorticity driven cavity solution using p finite elements*, Comput. Fluids **26**(1997), 453-468.
5. F. Brezzi and M. Fortin, *Mixed and Hybrid Finite Element Method*, Springer Verlag; New York,1991.
6. C. Carstensen and S. A. Funken, *A posteriori error control in low-order finite element discretisations of incompressible stationary flow problems*, Math. Comp **70**(2001), 1353-1381.

7. H. C. Elman, D. J. Silvester and A. Wathen, *Finite Elements and Fast Iterative Solvers with Applications in Incompressible Fluid Dynamics*, Oxford University Press, 2005.
8. S. Garcia, *The lid-driven square cavity flow: From stationary to time periodic and chaotic*, Commun. Comput. Phys **2** (2007), 900-932.
9. U. Ghia, K. Ghia, and C. Shin, *High Re solution for incompressible viscous flow using the Navier-Stokes equations and a multigrid method*, J. Comput. Phys **48**(1982), 387-395.
10. V. Girault, P. A. Raviart, *Finite Element Methods for Navier-Stokes Equations*, Springer-Verlag, Berlin, 1986.
11. P. Gresho, D. Gartling, J. Torczynski, K. Cliffe, K. Winters, T. Garratt, A. Spence, and J. Goodrich, *Is the steady viscous incompressible 2d flow over a backward facing step at Re = 800 stable?*, Int. J. Numer. Methods Fluids **17**(1993), 501-541.
12. V. John, *Residual a posteriori error estimates for two-level finite element methods for the Navier-Stokes equations*, Appl. Numer. Math **37**(2001), 503-518.
13. N. Kechkar and D. Silvester, *Analysis of locally stabilized mixed finite element methods for the Stokes problem*, Math. Comp **58** (1992), 1-10.
14. T. J. Oden, W. Wu, M. Ainsworth, *An a posteriori error estimate for finite element approximations of the Navier-Stokes equations*, Comput. Methods Appl. Mech. Engrg **111** (1994), 185-202.
15. M. U. Rehman, C. Vuik, *A comparison of preconditioners for incompressible Navier-Stokes solvers*, Int. J. Numer. Meth. Fluids **57** (2007), 1731-1751.
16. R. Verfurth, *A posteriori error estimators for the Stokes equations*, Numer. Math **55**(1989), 309-325.
17. R. Verfurth, *A Review of a posteriori Error Estimation and Adaptive Mesh-Refinement Techniques*, Wiley-Teubner, Chichester, 1996.
18. D. BH. Wu and I. G. Currie, *Analysis of a posteriori error indicator in viscous flows*, Int. J. Num. Meth. Heat Fluid Flow **12**(2001), 306-327.
19. G. O. C. Zienkiewicz, R.L.Taylor δ P. Nithiarasu, *The Finite Element Method for Fluid Dynamics*, Sixth edition.Elsevier Butterworth-Heinemann, 2005.

Abdeslam Elakkad Laboratoire Génie Mécanique, Faculté des Sciences et Techniques, B.P. 2202, Route d'Imouzzer, Fès Morocco.
`e-mail: elakkadabdeslam@yahoo.fr`

Ahmed Elkhalfi Laboratoire Génie Mécanique, Faculté des Sciences et Techniques, B.P. 2202, Route d'Imouzzer, Fès Morocco.
`e-mail: aelkhalfi@gmail.com`

Najib Guessous Département de mathématiques et informatique, Ecole normale Supérieure de Fès, B.P. 5206, Bensouda, Fès, Morocco.
`e-mail: ngessous@yahoo.fr`